6th Annual International IEEE EMBS Conference on Neural Engineering
San Diego, California, 6 - 8 November, 2013

State and trajectory decoding of upper extremity movements from electrocorticogram

Po T. Wang[1], Eric J. Puttock[2], Christine E. King[1], Andrew Schombs[1], Jack J. Lin[3], Mona Sazgar[3], Frank P.K. Hsu[4], Susan J. Shaw[5,6], David E. Millett[5,6], Charles Y. Liu[7,8], Luis A. Chui[3], An H. Do[3], and Zoran Nenadic[1,9]

Abstract— **Electrocorticography has been widely explored as a long-term signal acquisition platform for brain-computer interface (BCI) control of upper extremity prostheses. However, a comprehensive study of elementary upper extremity movements and their relationship to electrocorticogram (ECoG) signals has yet to be performed. This study examines whether kinematic parameters of 6 elementary upper extremity movements can be decoded from ECoG signals in 3 subjects undergoing subdural electrode placement for epilepsy surgery evaluation. To this end, we propose a 2-stage decoding approach that consists of a state decoder to determine idle/move states, followed by a Kalman filter-based trajectory decoder. This proposed decoder successfully classified idle/move states with an average accuracy of 91%, and the correlation between decoded and measured trajectory averaged 0.70 for position and 0.68 for velocity. These performances represent an improvement over a simple regression-based approach.**

I. Introduction

Electrocorticogram (ECoG) has been increasingly studied as a potential signal acquisition platform for brain-computer interface (BCI) controlled upper extremity prostheses. Successful ECoG-based BCI systems require the ability to robustly decode movement kinematic parameters. Examples include the decoding of finger trajectories [1], [2], [3], [4], [5], [6], [7], elbow and hand movements [8], [9], and reaching directions [8], [10], [11], [12], [13].

With the exception of [2], [4], and [12], these decoders either omitted idling periods, or were unable to accurately predict idling periods. However, for practical BCI control, accurate prediction of idling periods is just as important as the detection of movement. In addition, the performance of many of these techniques, measured by the correlation between actual and decoded trajectories, were relatively modest (average: 0.32–0.64). Finally, these studies only examined limited degree-of-freedom (DOF) movements. To restore independence to a potential user, however, a BCI-controlled upper extremity prosthesis will require at least 6 DOFs [14].

Motivated by these shortcomings, the present study uses a 2-stage approach for upper extremity trajectory decoding. First, a binary decoder utilized μ, β, and γ ECoG bands to distinguish between idling and movement states. Second, a continuous decoder, constrained by a dynamic movement model, was used to recover movement trajectories during the movement states. The performance of the above method was tested on ECoG signals underlying 6 elementary upper extremity movements.

Work supported by the National Science Foundation (Award #1134575) and the National Institute of General Medical Sciences (Award #P50GM076516).

[1]Department of Biomedical Engineering, UCI, CA, USA {ptwang, kingce, aschombs, znenadic}@uci.edu
[2]MCB Gateway Graduate Program, Center for Complex Biological Systems, UCI, Irvine, CA, USA eputtock@uci.edu
[3]Department of Neurology, UCI, Irvine, CA, USA {and, jjlin, msazgar, lchui}@uci.edu
[4]Department of Neurosurgery, UCI, Irvine, CA, USA fpkhsu@uci.edu
[5]Department of Neurology, Rancho Los Amigos National Rehabilitation Center (RLANRC), Downey, CA, USA
[6]Department of Neurology, University of Southern California (USC), Los Angeles, CA, USA {millett, shaws}@usc.edu
[7]Department of Neurosurgery, RLANRC, Downey, CA, USA
[8]Department of Neurosurgery, USC, Los Angeles, CA, USA cliu@usc.edu
[9]Department of Electrical Engineering and Computer Science, UCI, Irvine, CA, USA

II. Methods

A. Signal Acquisition and Training Data Collection

This study was approved by the Institutional Review Boards of the University of California, Irvine and the Rancho Los Amigos National Rehabilitation Center. Subjects were recruited from a patient population undergoing epilepsy surgery evaluation. Recruitment was limited to those with standard subdural electrodes (1 cm apart) implanted over the upper extremity representation area of the primary motor cortex (M1). Up to 64 channels of ECoG data were recorded with a pair of linked Nexus-32 bioamplifiers (Mind Media, Roermond-Herten, The Netherlands), and these signals were acquired at 2048 Hz in a common average reference mode.

Similar to [15] and [16], subjects performed 6 elementary arm movements on the side contralateral to their ECoG grid: **1.** pincer grasp and release (PG); **2.** wrist flexion and extension (W); **3.** forearm pronation and supination (PS), **4.** elbow flexion and extension (E); **5.** shoulder forward flexion and extension (SF); **6.** shoulder internal and external rotation (SR). For each movement type, the subjects performed 4 sets of 25 continuous repetitions, with each set intervened by a 20–30 s idling period.

The trajectories of movements **1** and **2** were measured by a custom-made electrogoniometer [17], while movements **3-6** were measured by a gyroscope (Wii Motion Plus, Nintendo, Kyoto, Japan). The trajectory signals, including the position, θ, and velocity, $\dot{\theta}$, were acquired using an integrated microcontroller unit (Arduino, Smart Projects, Turin, Italy).

978-1-4673-1969-0/13/$31.00 ©2013 IEEE

Finally, the ECoG data were synchronized with the trajectory signals using a common pulse train.

B. Decoding Model Design

For each DOF, the decoding model consisted of a state decoder followed by a Kalman filter trajectory decoder.

1) State Decoder: ECoG signals were divided into consecutive non-overlapping 0.25 s windows. The logarithmic spectral powers were calculated for each window in the following bands: μ (8-12 Hz), β (13-30 Hz), low-γ (30-50 Hz), and high-γ (80-160 Hz). Taking the logarithm of the powers equalized the otherwise disparate power levels, especially between the μ and high γ bands. This avoided skewing the parameters of the state decoder.

The spectral powers were classified into idling and movement states by first performing feature extraction using a combination of classwise principal component analysis (CPCA) [18], [19] and approximate information discriminant analysis (AIDA) [20]. One-dimensional (1D) spatio-spectral features were extracted by:

$$f = T_A \Phi_C(d) \tag{1}$$

where $f \in \mathbb{R}$ is the feature, $d \in \mathbb{R}^{b\times c}$ are single-trial spatio-spectral ECoG data (b- the number of frequency bands, c-the number of channels), $\Phi_C : \mathbb{R}^{b\times c} \to \mathbb{R}^m$ is a piecewise linear mapping from the data space into the *m*-dimensional CPCA-subspace, and $T_A \in \mathbb{R}^{1\times m}$ is an AIDA transformation matrix. Then, a linear Bayesian classifier:

$$f^\star \in \begin{cases} \mathcal{I}, & \text{if} \quad P(\mathcal{I}\,|f^\star) > P(\mathcal{M}\,|f^\star) \\ \mathcal{M}, & \text{otherwise} \end{cases} \tag{2}$$

was designed in the feature domain, where $P(\mathcal{I}\,|f^\star)$ and $P(\mathcal{M}\,|f^\star)$ are the posterior probabilities of idling and movement classes, respectively, given the observed feature, $f^\star$. This entire procedure was performed for each movement, and the classified idle and movement state trajectories were estimated using the following trajectory decoder.

2) Kalman Filter-Based Trajectory Decoder: High-γ power envelopes, P, were derived from ECoG signals according to [16]. Briefly, ECoG were band-pass filtered (80-160 Hz), their instantaneous powers were calculated by squaring the signals, and the results were enveloped using a 0.5-sec Gaussian window. P was then used as the observation in the dynamic model below.

To facilitate Kalman filter development, the following dynamic model is assumed:

$$\begin{aligned} x_{k+1} &= Ax_k + w_k \\ y_k &= Cx_k + n_k \end{aligned} \tag{3}$$

where $x_k \in \mathbb{R}^{2\times 1}$ is the state consisting of the angular position, θ, and velocity, $\dot{\theta}$, k is the current time step, $A \in \mathbb{R}^{2\times 2}$ is the state matrix, and $w_k \sim \mathcal{N}(0, \Sigma_w)$ is zero-mean Gaussian process noise with covariance Σ_w. Similarly, $y_k \in \mathbb{R}^{c\times 1}$ is the output (note that $y_k = P_k$), $C \in \mathbb{R}^{c\times 2}$ is the output matrix, and $n_k \sim \mathcal{N}(0, \Sigma_n)$ is zero-mean Gaussian measurement noise with covariance Σ_n. Both A and C are computed from the data according to [21]. The Kalman filter was then constructed to compute the position and velocity at the next time step [21]:

$$\begin{aligned} \Sigma_{k+1} &= [I - L_{k+1}C]\left[A\Sigma_k A^{\mathrm{T}} + \Sigma_w\right] \\ L_{k+1} &= \left[A\Sigma_k A^{\mathrm{T}} + \Sigma_w\right] C^{\mathrm{T}} \left[C\left[A\Sigma_k A^{\mathrm{T}} + \Sigma_w\right] C^{\mathrm{T}} + \Sigma_n\right]^{-1} \end{aligned}$$

where Σ is the *a posteriori* error covariance and L is the optimal gain.

C. Performance Measure

The data were split into two halves, with one half used for training the state and trajectory decoders, and the other half used for validation. The above process was then repeated with the roles of the training and validation sets reversed. The decoder performance was assessed by comparing the reconstructed trajectories ($\hat{\theta}$, $\hat{\dot{\theta}}$) to the trajectories measured by the electrogoniometer or gyroscope (θ, $\dot{\theta}$). To this end, the fraction of correctly decoded idle and movement states, P_c, and the correlation coefficient of movement, ρ_M, were calculated. In addition, to judge the overall performance with a single number, the following Performance Measure, PM, was used:

$$\text{PM} = \frac{\rho_M n_M + P(I|I) n_I}{n_M + n_I} \times 100\% \tag{4}$$

where n_M and n_I is the number of movement and idle state samples, respectively, and $P(I|I)$ is the probability of correctly decoding the idling state.

III. Results

Three subjects were recruited for the study. Their demographics and ECoG electrode locations are summarized in Table I. A representative ECoG electrode location map can be seen in Fig. 1. The probability of correct state decoding, P_c, movement correlation coefficients, ρ_M, and performance measures, PM, for position, θ, and velocity, $\dot{\theta}$, are summarized in Table II. It can be seen in Table II that there are two numbers for each measure, one for each validation set. Note that the probability of correct state decoding, P_c, is the same for both position and velocity since it was determined from the same state decoder.

TABLE I
SUBJECT DEMOGRAPHICS AND GRID LOCATION/SIZE.

Subject	Sex	Age	Grid Size	Grid Location
1	F	20	8×8 grid, 1×6 strip	Left temporal-frontal, Posterior-frontal
2	F	27	6×8 grid	Right frontal-parietal
3	F	35	2×6 strip	Right frontal-parietal

The representative trajectory decoding results for the pincer grasp movement of Subject 3 are shown in Fig. 2. Note that for the periods classified as idle, the position was held constant, while the decoded velocity was set to 0.

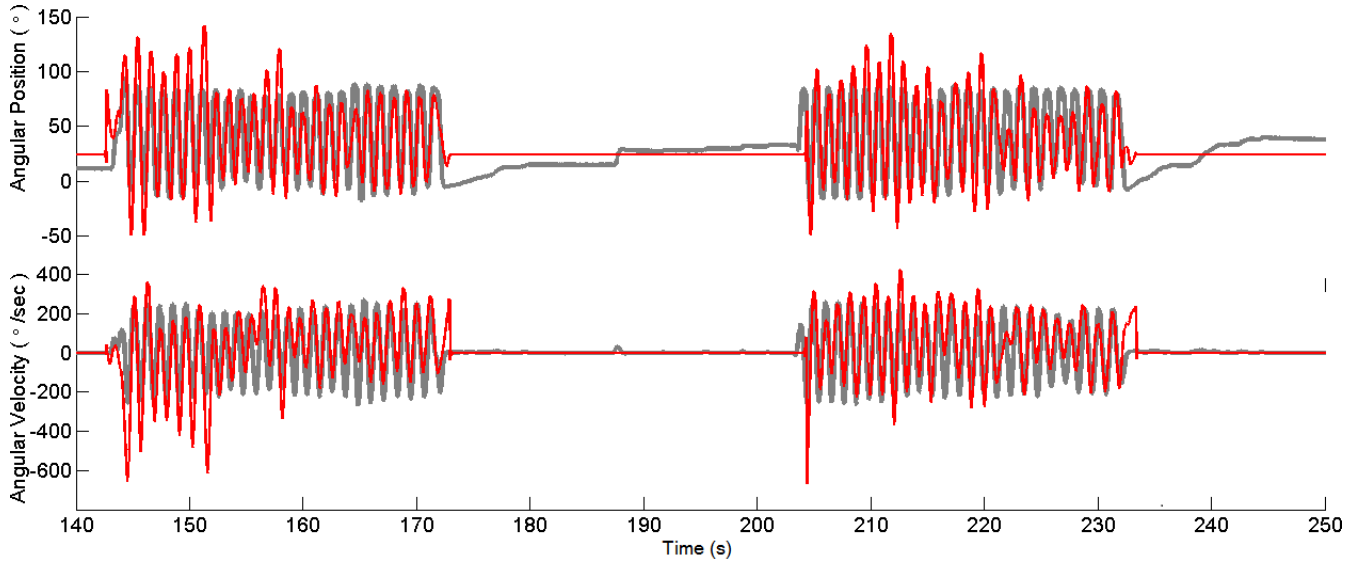

Fig. 2. Representative ECoG-decoded (red thin line) and measured (gray thick line) velocities during pincer grasping for Subject 3.

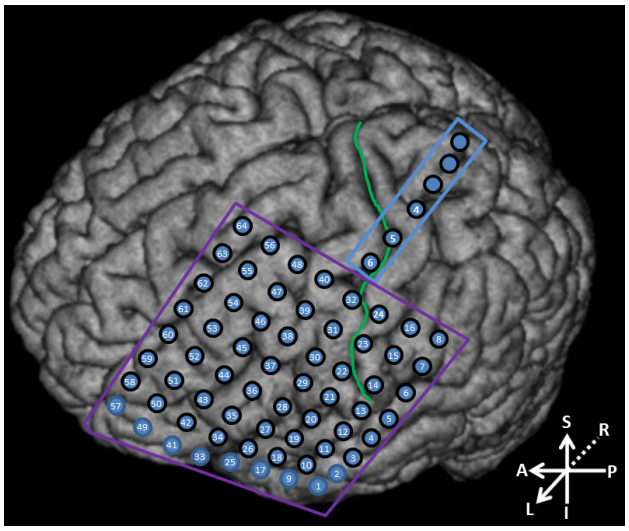

Fig. 1. Representative electrode grid placement (Subject 1).

TABLE II

TRAJECTORY DECODING RESULTS FOR EACH SUBJECT S: MOVEMENTS, M; PROBABILITY OF CORRECT STATE DECODING, P_c; CORRELATION COEFFICIENT OF MOVEMENT, ρ_M; AND PERFORMANCE MEASURE, PM.

S	M	P_c (%)	ρ_M Pos.	PM Pos. (%)	ρ_M Vel.	PM Vel. (%)
1	PG	79, 95	0.40, 0.39	71, 64	0.29, 0.49	66, 69
	W	90, 98	0.71, 0.69	76, 78	0.68, 0.67	75, 77
2	PG	90, 81	0.78, 0.56	76, 71	0.76, 0.55	75, 71
	E	90, 85	0.71, 0.66	68, 77	0.68, 0.67	65, 77
	SR	93, 96	0.76, 0.86	78, 89	0.74, 0.84	76, 88
	SF	96, 89	0.82, 0.70	85, 80	0.81, 0.72	84, 82
3	PG	91, 98	0.86, 0.83	86, 91	0.80, 0.76	83, 87
Avg.		90, 92	0.72, 0.67	77, 79	0.68, 0.67	75, 79

To gauge the performance of these results, they were compared to our previously reported regression-based approach [16]. Briefly, this approach used a linear regression model between the instantaneous power in the high γ band and the known velocity to classify idle and movement states. Similar to the present approach, the velocity during states decoded as idling was set to 0. Conversely, the velocity during states decoded as movement was estimated using a 2nd linear regression model. These prior results are reproduced in Table III for comparison purposes. Note that since the regression-based approach was only applied to the velocity decoding [16], the decoded positions are not reported.

TABLE III

THE PROBABILITY OF CORRECT STATE DECODING, P_c, AND THE CORRELATION COEFFICIENT, ρ_M, BETWEEN ACTUAL AND DECODED MOVEMENT VELOCITY USING THE REGRESSION-BASED APPROACH [16].

S	M	P_c (%)	ρ_M
1	PG	81, 85	0.66, 0.68
	W	83, 89	0.52, 0.46
2	PG	89, 73	0.62, 0.54
	E	80, 80	0.53, 0.44
	SR	80, 68	0.53, 0.62
	SF	87, 82	0.69, 0.53
3	PG	88, 89	0.80, 0.76
Avg.		84, 81	0.60, 0.56

IV. DISCUSSION

With the exception of the pronation/supination movement, this study demonstrates that movements of multiple upper extremity joints can be decoded from ECoG signals with a reasonably high accuracy. The state decoder classified idle and movement states with a high probability (average ~91%). A notable exception to this is the PG movement in Subject 1, where a relative drop in decoding performance

was observed. Also, the proposed state decoder outperformed the regression-based approach by a wide margin (average $\sim$83%). Since the regression-based approach only utilizes the high-γ band, these results also suggest that significant information about the movement state can be gleaned from the μ, β and low-γ bands.

The position and velocity of upper extremity movements were accurately decoded by the Kalman filter, as evidenced by the average correlation of 0.70 (position) and 0.68 (velocity). This represents a significant improvement with respect to velocity decoding using the simple linear regression approach (average $\rho_M = 0.58$). These results are not surprising given that the dynamic model (3) imposes smoothness constraints on the decoded trajectories, ultimately resulting in a higher decoding accuracy. Note that both the Kalman filter and the linear regression-based trajectory decoder only utilized the high-γ band, and that the addition of other frequencies generally degraded the performance.

Despite these relatively accurate results, there are several instances when the decoded trajectory overshoots the measured trajectory. This may be problematic when developing a BCI-driven upper extremity prosthesis, as the prosthesis itself will have physical constraints. The overshoot could be mitigated by imposing boundary conditions that conform to the physical constraints of the prosthesis.

In summary, the relatively high state and trajectory decoding accuracies resulted in average performance measures of 78% (position) and 77% (velocity). Additionally, the approach here was successfully applied to multiple DOFs of the upper extremities, especially in the case of Subject 2 (4 out of 6). The ability to decode multiple DOF movements was largely determined by the grid placement, which also explains why Subject 1 and Subject 3 had only 2 and 1 DOF movements decoded, respectively. Furthermore, the present study only examined the decoding of one DOF movement at a time. Our prior work indicates that resolving movement states of multiple joints may be challenging [15], as sensitivity (idling vs. moving) and specificity (which joint is moving) are generally traded off. It therefore remains unclear to what degree this is true of trajectory decoding. Nevertheless, the preliminary success reported here warrants additional investigation, possibly with higher resolution signals, such as mini- or micro-ECoG grids.

V. Conclusion

The findings here suggest that the power of the ECoG high-γ band can be used to accurately decode both the state and trajectory information from ECoG signals for several individual movement types. The ability to accurately decode these movements may lead to BCI control of a 6 DOF upper extremity prosthesis, however, additional research must be performed to resolve the individual movements and facilitate proper BCI-control of an upper extremity prosthesis.

VI. Acknowledgements

The authors acknowledge Angelica Nguyen and Christel Jean for their help in setting up the experiments.

References

[1] G. Schalk, J. Kubánek, K.J. Miller, N.R. Anderson, E.C. Leuthardt, J.G. Ojemann, D. Limbrick, D. Moran, L.A. Gerhardt, and J.R. Wolpaw. Decoding two-dimensional movement trajectories using electrocorticographic signals in humans. *J Neural Eng*, 4(3):264–275, 2007.

[2] K.J. Miller, S. Zanos, E.E. Fetz, M. den Nijs, and J.G. Ojemann. Decoupling the cortical power spectrum reveals real-time representation of individual finger movements in humans. *J Neurosci*, 29(10):3132–3137, 2009.

[3] J. Kubánek, K.J. Miller, J.G. Ojemann, J.R. Wolpaw, and G. Schalk. Decoding flexion of individual fingers using electrocorticographic signals in humans. *J Neural Eng*, 6(6):66001, 2009.

[4] Z. Wang, Q. Ji, K.J. Miller, and G. Schalk. Prior knowledge improves decoding of finger flexion from electrocorticographic signals. *Front Neurosci*, 5:127, 2011.

[5] N. Liang and L. Bougrain. Decoding finger flexion from band-specific ecog signals in humans. *Front Neurosci*, 6:91, 2012.

[6] S. Acharya, M.S. Fifer, H.L. Benz, N.E. Crone, and N.V. Thakor. Electrocorticographic amplitude predicts finger positions during slow grasping motions of the hand. *J Neural Eng*, 7(4):046002, 2010.

[7] H.L. Benz, H. Zhang, A. Bezerianos, S. Acharya, N.E. Crone, Xioaxiang Zheng, and N.V. Thakor. Connectivity analysis as a novel approach to motor decoding for prosthesis control. *IEEE Trans. Neural Syst. Rehab. Eng.*, 20(2):143–152, 2012.

[8] C.M. Chin, M.R. Popovic, A. Thrasher, T. Cameron, A. Lozano, and R. Chen. Identification of arm movements using correlation of electrocorticographic spectral components and kinematic recordings. *J Neural Eng*, 4(2):146–158, 2007.

[9] T. Yanagisawa, M. Hirata, Y. Saitoh, H. Kishima, K. Matsushita, T. Goto, R. Fukuma, H. Yokoi, Y. Kamitani, and T. Yoshimine. Electrocorticographic control of a prosthetic arm in paralyzed patients. *Ann Neurol*, 71(3):353–361, 2012.

[10] T. Pistohl, T. Ball, A. Schulze-Bonhage, A. Aertsen, and C. Mehring. Prediction of arm movement trajectories from ECoG-recordings in humans. *J Neurosci Methods*, 167(1):105–114, 2008.

[11] J.C. Sanchez, A. Gunduz, P.R. Carney, and J.C. Principe. Extraction and localization of mesoscopic motor control signals for human ecog neuroprosthetics. *J Neurosci Meth*, 167(1):63–81, 2008.

[12] Z. Wang, A. Gunduz, P. Brunner, A.L. Ritaccio, Q. Ji, and G. Schalk. Decoding onset and direction of movements using electrocorticographic (ECoG) signals in humans. *Front Neuroeng*, 5:15, 2012.

[13] S. Kellis, S. Hanrahan, T. Davis, P.A. House, R. Brown, and B. Greger. Decoding hand trajectories from micro-electrocorticography in human patients. In *Proc 34th IEEE EMBS Int'l Conf*, pages 4091–4094, 2012.

[14] D.P. Romilly, C. Anglin, R.G. Gosine, C. Hershler, and S.U. Raschke. A functional task analysis and motion simulation for the development of a powered upper-limb orthosis. *IEEE Trans. Rehab. Eng.*, 2(3):119–129, 1994.

[15] A.H. Do, P.T. Wang, C.E. King, A. Schombs, J.J. Lin, M. Sazgar, F.P.K. Hsu, S.J. Shaw, D.E. Millett, C.Y. Liu, A.A. Szymanska, L.A. Chui, and Z. Nenadic. Sensitivity and specificity of upper extremity movements decoded from electrocorticogram. In *Proc 35th IEEE EMBS Ann Int'l Conf*, pages 5618–5621, 2013.

[16] P.T. Wang, C.E. King, A. Schombs, J.J. Lin, M. Sazgar, F.P.K. Hsu, S.J. Shaw, D.E. Millett, C.Y. Liu, Z. Nenadic, and A.H. Do. Electrocorticographic gamma band power encodes the velocity of upper extremity movements. In *Proc 5th Int'l Brain-Computer Interface Meeting*, Article ID 120, 2013.

[17] P.T. Wang, C.E. King, A.H. Do, and Z. Nenadic. A durable, low-cost electrogoniometer for dynamic measurement of joint trajectories. *Med Eng Phys*, 33(5):546–552, 2011.

[18] K. Das, S. Osechinskiy, and Z. Nenadic. A classwise PCA-based recognition of neural data for brain-computer interfaces. In *Proc 29th IEEE EMBS Ann Int'l Conf*, pages 6519–6522, 2007.

[19] K. Das and Z. Nenadic. An efficient discriminant-based solution for small sample size problem. *Pattern Recogn*, 42(5):857–866, 2009.

[20] K. Das and Z. Nenadic. Approximate information discriminant analysis: A computationally simple heteroscedastic feature extraction technique. *Pattern Recogn*, 41(5):1548–1557, 2008.

[21] W. Wu, Y. Gao, E. Bienenstock, J.P. Donoghue, and M.J. Black. Bayesian population decoding of motor cortical activity using a Kalman filter. *Neural Comput*, 18:80–118, 2006.